Dynamics of nucleosomal structures measured by high-speed Atomic Force Microscopy

*Allard J. Katan, Rifka Vlijm, Alexandra Lusser and Cees Dekker**

This is the author-edited copy of the paper that appeared in Small (online publication date 21 October 2014). The published version can be found here:
http://dx.doi.org/10.1002/smll.201401318

Keywords: single-molecule studies, DNA, atomic-force microscopy, nucleosome dynamics

Abstract:

The accessibility of DNA is determined by the number, position, and stability of nucleosomes, complexes consisting of a core of 8 histone proteins with DNA wrapped around it. Since the structure and dynamics of nucleosomes affects essential cellular processes, they are the subject of many current studies. Here we use high-speed Atomic Force Microscopy to visualize dynamic processes in nucleosomes and tetrasomes (subnucleosomal structures that contain 4 rather than 8 histones in the protein core). We find that nucleosomes can spontaneously disassemble in a process (at a 1 second timescale). For tetrasomes we observe multiple dynamic phenomena. For example, during disassembly we observe the formation of a DNA loop (~25 nm in length) which remains stable for several minutes. For intact tetrasomes, we observe dynamics in the form of sliding and reversible hopping between stable positions along the DNA. The data emphasize that tetrasome are not merely static objects but highly dynamic. Since tetrasomes (in contrast to nucleosomes) can stay on the DNA during transcription, the observed tetrasome dynamics is relevant for our understanding of the nucleosomal dynamics during transcription. Our results illustrate the diversity of nucleosome dynamics and demonstrate the ability of high speed AFM to characterize protein-DNA interactions.

1. Introduction

DNA in eukaryotic cells is strongly condensed to fit into the nucleus. Perhaps counterintuitively, histone proteins are added to compact DNA into nucleosomes. Each nucleosome is built up of 50nm of DNA (147 bp) that is wrapped 1.7 times around a protein-disk consisting of a histone octamer [1]. Nucleosome packaging provides compaction, but also results in a decrease of DNA accessibility, which affects many important processes in the cell, like DNA transcription, replication, and repair. Therefore the number and position of nucleosomes is highly regulated by chromatin remodeling complexes.

In cells, two copies each of histones H2A, H2B, H3 and H4 are collected by histone chaperones such as the nucleosome assembly protein 1 (NAP1) and chromatin remodelers, to enforce the correct binding order of histones onto the DNA [2]. First, histones H3 and H4 form a tetrasome $(H3\text{-}H4)_2$ on DNA, followed by the binding of histones H2A and H2B to complete the nucleosome $(H2A\text{-}H2B\text{-}H3\text{-}H4)_2$ on DNA. Once formed, nucleosomes are not static: they can reposition [3], (spontaneously)

Dr. A. J. Katan, Dr. R. Vlijm, Prof. Dr. C. Dekker :
Bionanoscience Department, Kavli Institute of Nanoscience, Delft University of Technology, Lorentzweg 1, 2628 CJ, The Netherlands
E-mail: C. Dekker @TUDelft.nl

Prof. Dr. A. Lusser
Division of Molecular Biology, Innsbruck Medical University,
Innrain 80-82, A-6020 Innsbruck, Austria

breath [4] (i.e., partially unwrap and rewrap), histones can be replaced [5, 6], and - to allow transcription machinery to move along the DNA - histones H2A and H2B have to be removed leaving only the $(H3\text{-}H4)_2$ tetrasomes attached to the DNA [7, 8]. Much less is known about the dynamics of tetrasomes, while better understanding of that would improve our understanding of how nucleosome structure affects transcription and vice versa.

Since the structure and dynamics of nucleosomes play such an important role it is subject to many recent studies. Binding affinities of histone proteins can be determined from biochemical experiments [9, 10]. These bulk assays, however, average over the population and in time. Using single-molecule techniques such as magnetic or optical tweezers, the dynamics of protein-induced DNA compaction can be studied at the molecular scale [11-13]. There are, however, many aspects of DNA-protein interactions that cannot be studied by means of magnetic or optical tweezers. For example, events that do not actively generate a force or torque on the DNA do not generate any observable changes in such tweezers. This includes the binding of many classes of proteins to DNA, diffusion of proteins along the DNA, and interactions of proteins bound to DNA with molecules in solution. When tweezers are combined with fluorescence microscopy [14], some of these processes can become observable, but the optical resolution is far from sufficient to resolve many of the molecular details. Furthermore, attaching fluorescent labels to the proteins of interest can be cumbersome and detrimental to function.

Atomic Force Microscopy (AFM) [15, 16] has the highest resolution of any microscopy technique when imaging in aqueous solutions. Until recently, the time resolution of AFM was poor, with typically several minutes to collect one image. This clearly is not sufficient to resolve nucleosome dynamics, where the relevant time scale was shown to in the order of 1 second in yeast [17]. Recent developments however, have increased the time resolution of AFM imaging in liquid to the range of an image acquisition time of <0.1 s per frame [18, 19].

Here, we apply such high-speed AFM to visualize the spontaneous dynamics of nucleosome and subnucleosomal assemblies. We observe that nucleosomes and tetrasomes can spontaneously disassemble through different pathways. Our study of tetrasomes reveals a rich dynamics, demonstrating, among other things, that they can exhibit sliding or 'hopping' between two distinct locations along the DNA.

2. Results and discussion

2.1 Spontaneous nucleosome disassembly

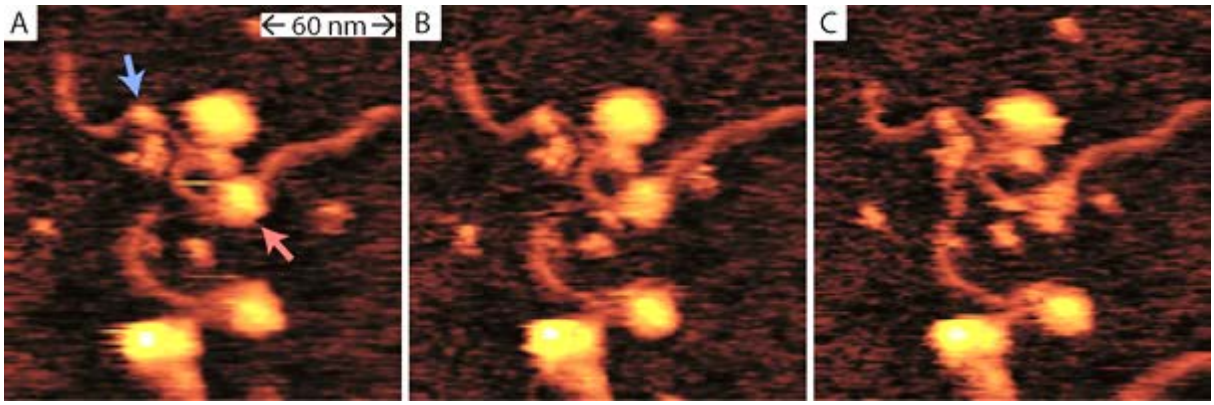

Figure 1: A-C: consecutive image series acquired at 1 s per frame of a nucleosome, indicated in A with a red arrow, falling apart. The large feature above the nucleosome is not attached to the DNA molecule. Residual protein that is still bound to the DNA after the nucleosome fell apart is indicated by the blue arrow.

Nucleosomes were assembled by the salt dialysis procedure described in the experimental section and deposited onto a lipid bilayer composed of a 1:1 mixture of DOPC/18:1 EPC. Concentration of DNA in the nucleosome sample was 0.2 ng μl^{-1} and sample was incubated 12 minutes before washing with imaging buffer. AFM scanning of these nucleosomes showed that they are instable under imaging conditions. Initially, DNA molecules with several nucleosomes on them could be identified. The apparent height of the nucleosomes is 4.5-5 nm, which can clearly be distinguished from tetrasomes, which are typically 2.5-3 nm in apparent height. During the imaging, the nucleosomes increasingly fell apart, leaving bare DNA molecules behind, as can be seen in Figure 1, which is composed of three frames of an AFM movie that is available in its entirety as Supplementary Movie 1. In Figure 1A, the nucleosome in the center of the image is still intact, but 1 second later, in Figure 1B, it has slightly shrunk to 4 nm in height, although it has not changed in width. Yet one second later, the nucleosome is reduced to multiple small protein clusters, presumably individual histones or histone dimers, that are only 2-2.5 nm high, and which dissociate from the DNA and diffuse away in subsequent images. The release of these small units from the DNA is often much slower than the disintegration of the nucleosome. They can remain for tens to hundreds of seconds on the DNA at the former position of the nucleosome. In Figure 1A, one such protein unit is indicated with a blue arrow. To check whether the AFM tip induced the instability of the nucleosomes, we also did an experiment where the tip was taken off the surface some time (up to

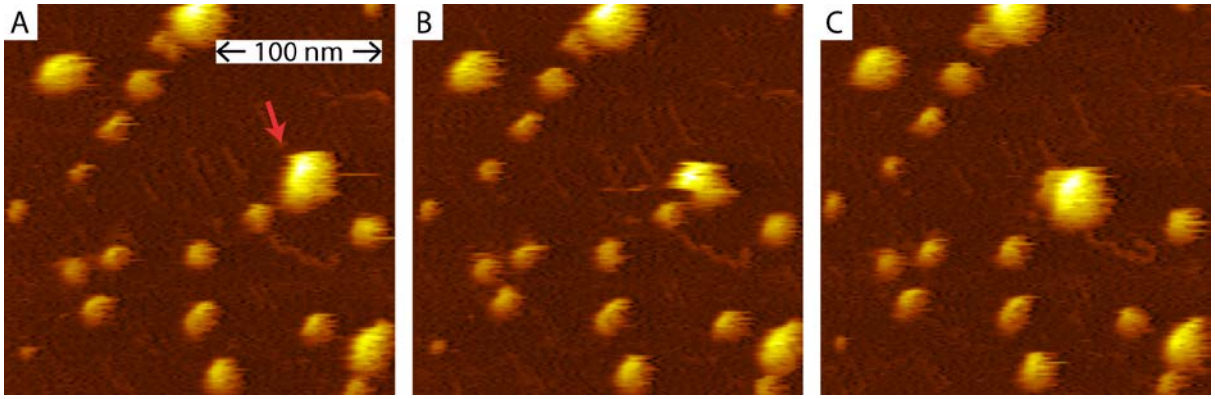

Figure 2: Surface aggregates formed after the NAP1 nucleosome-assembly protocol. A cluster of approximately 8 nm height moves over the surface to merge with a smaller cluster.

several minutes) between scans, which showed that nucleosomes were spontaneously removed even without contact with the AFM tip. From the experiments, we found that even though nucleosomes can remain intact for tens of minutes after deposition, once the disassembly starts, it is completed in ~1 second or less. Suzuki *et al.* [20] also reported spontaneous disruption of individual nucleosomes in reconstituted nucleosome arrays, with a time scale similar to our experiments. Though they do see on rare occasions that the fast dissociation occurs in two steps about one second apart, the occurrence of small protein clusters that remain associated with DNA for tens of seconds after the nucleosome has fallen apart was not reported in their work. We did not see evidence of loops of DNA forming close to the nucleosome prior to complete disassembly, as was reported earlier in high-speed AFM measurements on nucleosomes [21].

2.2 Surface aggregation of histones during AFM scanning

For nucleosomes assembled by use of the assembly chaperone NAP1, small clusters can be seen on the surface in cases where the NAP1-histone ratio was not optimal. Usually these clusters were found to aggregate further during the imaging. Figure 2 depicts such an event, which can also be seen as a movie in Supplementary Movie 2. A large protein cluster can be seen to move over the surface and 'swallow' a smaller cluster. Once aggregates were formed they seldomly disintegrated spontaneously. High scanning forces greatly speeded up the aggregation, presumably by increasing the surface mobility of the histone clusters beyond purely diffusive motion. It is important to distinguish events like the aggregation shown in Figure 2 one from steps in the nucleosome assembly process, such as the addition of an H2A-H2B dimer to an H3H4-DNA tetrasome. A clear clue for the distinction is provided by the size of the aggregation clusters, which has a broad distribution and includes clusters of

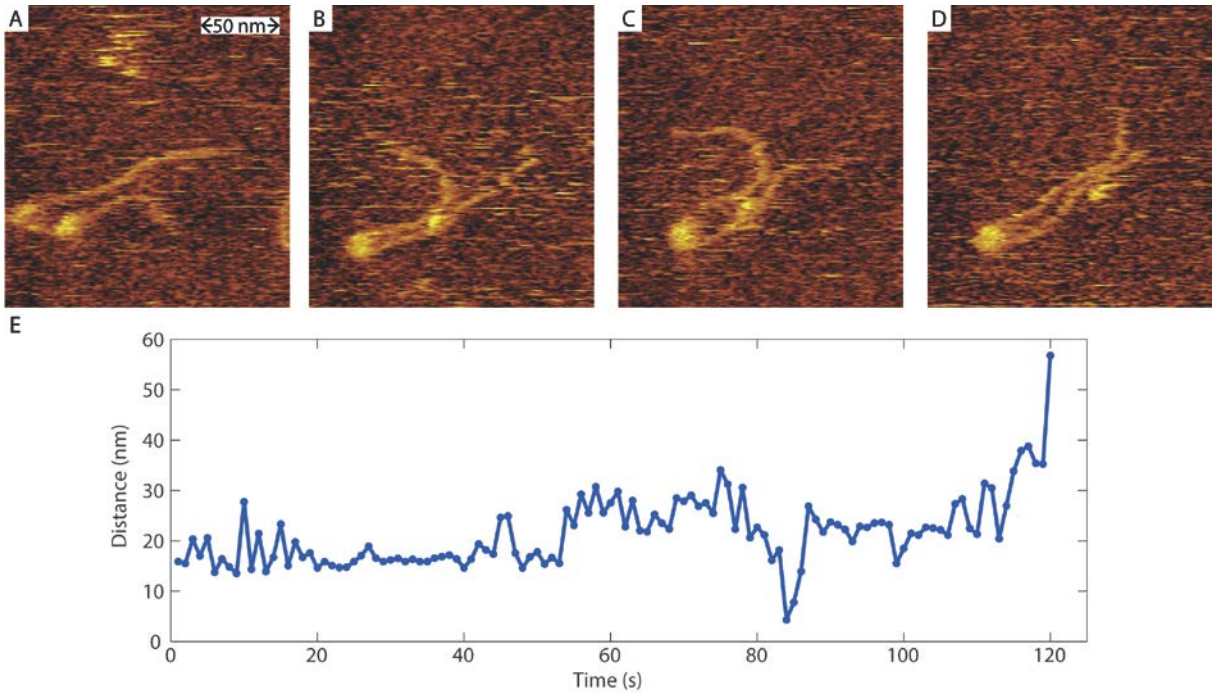

Figure 3: Tetrasome sliding along DNA. A-D: individual snapshots at t=64, 112, 116 and 118 s respectively. E: Time trace of the distance between two tetrasomes along a double stranded DNA molecule. Out of two tetrasomes on the same DNA molecule, one stays attached (remaining attached for at least 300s of imaging with no detectable shift in position on the DNA), while the other one shows significant motion along the DNA followed by dissociation after 120 s of imaging.

10 nm or higher. In contrast, NAP1-histone complexes that we imaged separately were found to have an apparent height of 4.5 ± 0.5 nm under typical AFM imaging conditions.

2.3 Dynamics of tetrasomes

2.3.1 Sliding of tetrasomes

A solution with tetrasomes assembled on 595 bp DNA by salt dialysis was diluted to 1.4 ng/µl DNA concentration and incubated for 1 minute on mica treated with Mg2+ (see experimental section). This lead to a surface covered with DNA molecules at a density of 50±20/µm^2, with the majority of molecules carrying one tetrasome. The surface mobility of the protein-DNA complexes was diverse even within a single sample preparation. Some complexes stayed in the same position and configuration for more than ten minutes of continuous high-speed imaging, where others would diffuse through the field of view with a speed of several tens of nm/s. Nevertheless, the majority of complexes was attached in such a way that they could be imaged for tens to hundreds seconds, while both DNA and protein were still able to change position frequently within this time. The high mobility of the DNA shows that surface influences are minimized. Nevertheless, it makes continuous accurate determination of position of the DNA ends – and thereby the exact position of the tetrasomes along the sequence - difficult. Figure 3A-D shows several snapshots of Supplementary Movie 3, in which we see a DNA molecule with two tetrasomes on it. This configuration is much less commonly found than a single tetrasome, but it simplifies the analysis since the relative position of the two tetrasomes can be measured accurately. The two tetrasomes move over the surface with the DNA, but at the same time their mutual distance (Figure 3E) is observed to change in a range of up to ~40 nm which shows that at least one of the tetrasomes slides along the DNA. The speed of this sliding reaches up to 42 bp/s, which illustrates how dynamic tetrasomes can be even in the absence of remodelers or other proteins. After two minutes, one of the two histone tetramers comes off the DNA and disappears from view. High-speed AFM measurements reported by the Takeyasu group [20] showed that complete nucleosomes can display a similar sliding behavior.

2.3.2 Hopping of tetrasomes between stable positions

After successful assembly of tetrasomes using the NAP1 assembly protocol described in the experimental section, samples were deposited on mica. After 5 minutes of incubation, they were rinsed and imaged in imaging buffer without crowding agents. Typically, AFM images showed that samples contain a mix of tetrasomes, bare DNA, and protein clusters not associated with DNA. Several tetrasomes were selected for closer examination of their dynamic behavior.

An example of such behavior is depicted in Figure 4, which show a DNA molecule with a tetrasome attached to it. The tetrasome is identified by its shape, the apparent height of 2.5 nm and the shortening of the DNA molecule by 25 nm from its expected contour length. Between the images in Figure 4B and C, the tetrasome is observed to hop between two positions in the image, which are located at different locations along the long axis of the DNA molecule. Image analysis of all 238 consecutive frames of Supplementary Movie 4 shows that, surprisingly, this change in position is reversible, as multiple hops between two stable positions are observed. A Gaussian fit to a histogram of the tetrasome position shows that these positions are approximately 3.6 nm apart. The DNA molecule is clearly very weakly adhered to the surface, as the ends can be seen to detach from the surface, e.g. the bottom end in Figure 4D, which attaches again in later images.

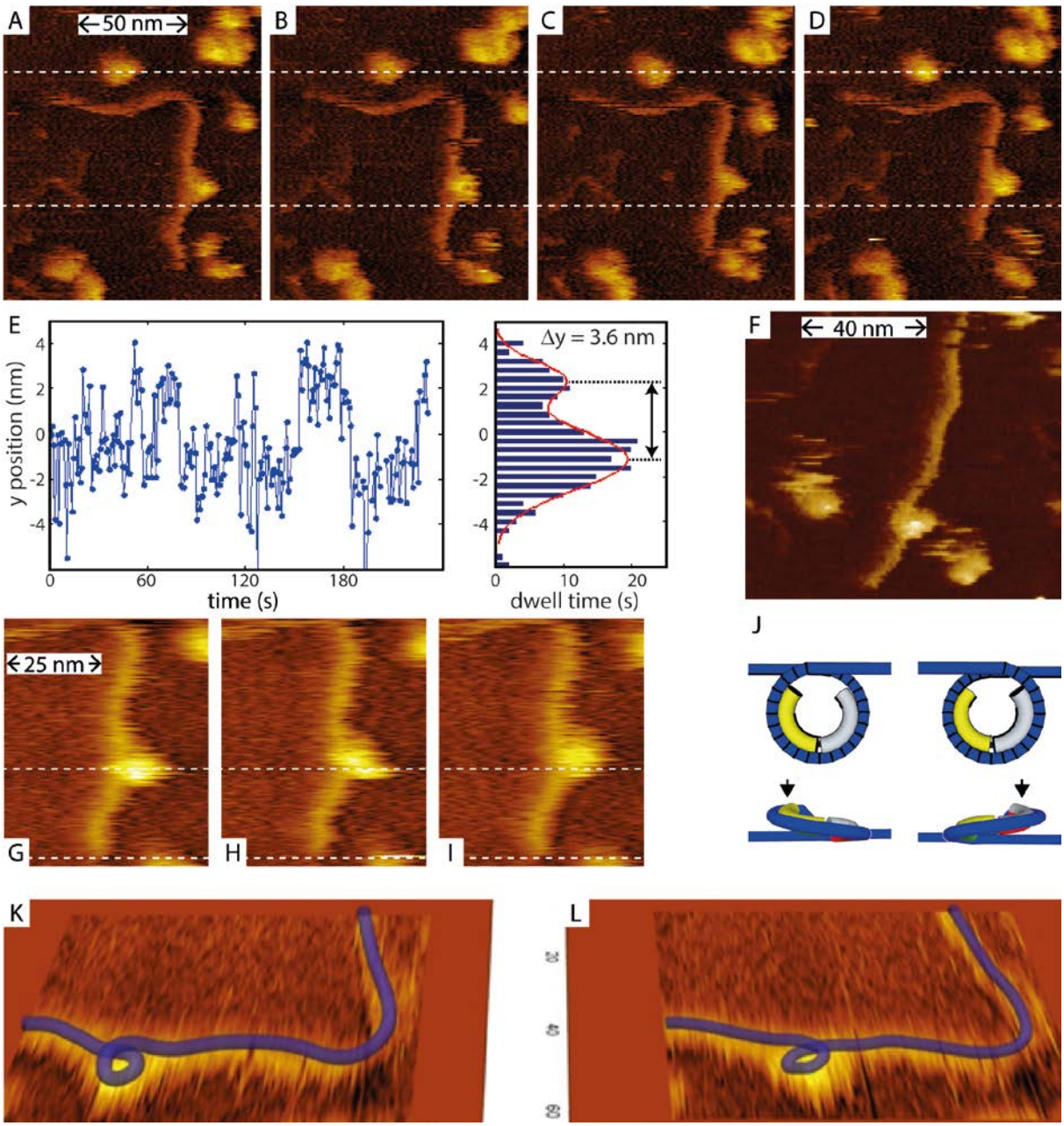

Figure 4: Tetrasome hopping/flipping on 595 bp DNA. A-D: Image series with excerpts from a 238 s movie acquired at 1 s per frame, of a tetrasome moving along a DNA molecule. Between the second and third image, the position of the tetrasome shifts upwards. White dashed lines are guides to the eye. The top white line goes through a feature that was stationary for the duration of the measurement and serves as a marker for position measurement. E: Time trace of the vertical position coordinate of the tetrasome in the entire movie, and a dwell time histogram. Images A-D correspond to the transition around t=152 s. A two-peak Gaussian fit (red line) shows that the peaks in the dwell time histogram are 3.6 nm apart. F: slower high-resolution image, acquired in 2 s, of the tetrasome. G-I: High-speed image series acquired at 0.3 s per frame, with excerpts from a 346 frame movie. Images are aligned to the lower edge of the DNA (lower dashed white line). In H, the transition from the lower to the higher state can be seen to occur. J: Top: Top view, bottom: side view of an artist impression of two rotational states of the tetrasomes (yellow/white/green and red indicate the H3-H4 tetramer, blue is the DNA). Arrows depict the highest point with respect to the surface in each state. K,L Artist impression of two rotational states of the tetrasomes and their possible correspondence to AFM images. The DNA molecule remains fixed in most places, but the rotational flipping changes the position where the DNA strand crosses itself, which alters the highest point. The background AFM

This raises the question whether the change in position of the tetrasome within the image occurs as a result of a sliding of the entire DNA molecule on the surface, or that the tetrasome moves with respect to the DNA. A more zoomed-in movie with a higher frame rate, available as Supplementary Movie 5, of which 3 frames are shown in Figure 4G-I, proves that the DNA end remains in the same position during the hop. Furthermore, the more frequently visited position is lower in the image, which indicates that it is highly unlikely that the position changes are caused by pushing with the AFM tip, as the slow scan direction is from bottom to top.

Two mechanisms could lead to the particular hopping that we observe: a sliding of the tetrasome (i.e. a translocation along the DNA helix), or a flipping motion where the position of the histones on the DNA is fixed, but the looping of the DNA around the histones changes its handedness. Sliding of full nucleosomes assembled onto the strong '601' positioning sequence has been reported with AFM by the Lyubchenko group [21], who reported irreversible sliding over 50 nm distances (in presence of the detergent CHAPS), as well as a reversible sliding between two positions 10 nm apart. However, the latter had only a single datapoint at one of the positions, while the nucleosome spent nearly all its time on the other position. This is not surprising given the presence of a strong positioning sequence. In our case however, there is no positioning sequence, which begs the question why there would be stable positions at all. Both our own data on tetrasome sliding (see section 2.3.1), as well as the results of Suzuki et al [20] show that once sliding is initiated, much longer distances are travelled. On another note: although our hopping distance of 3.6nm is similar to the distance between two contact points of DNA with the octamer surface in a nucleosome [1, 22], there is no reason to assume sliding is kinetically hindered at a particular location, so a repeated sliding back and forth between only two attachment points is not expected.

The hopping between two stable positions can however be explained as the rotational flipping of a tetrasome. Based on the observation that tetrasomes with a positive chirality occur on DNA with positive torque and tetrasomes with negative chirality on DNA with negative torque, flipping in the handedness of tetrasomes was previously proposed [23]. Such a mechanism could have profound implications for transcription. During transcription, the outer histones H2A and H2B have to be removed in order to allow the transcription machinery to move along the DNA [7, 8, 24]. A well-known problem during transcription, is the expected buildup of torque ahead and behind the moving transcription machinery [25]. Flipping of $(H3\text{-}H4)_2$ tetramers could absorb some of this induced supercoiling, preventing extreme buildup of torque that would interfere with the correct function of many motor proteins. The suggested model of flipping tetrasomes thus would explain an important part of the robustness of transcription. However, so far no direct observation has been made that a single tetrasome indeed can change chirality. Our study of the dynamics of tetrasomes leads to the interesting results of repeatable 'hopping' of a single tetrasome between two distinct locations along the DNA, separated by 3.6nm. We interpret this as the rotational flipping of a tetrasome as predicted by the previous model and in agreement with very recent, yet unpublished, results of magnetic tweezers experiments [26] that indicate that NAP1-assembled tetrasomes on DNA (without positioning sequences) can flip between two rotational states, that have different handedness with a linking number change of 1.7 turns. Figure 4J-L illustrates how such a flipping motion could lead to the observed change in position. The change in handedness of the tetrasome flips the maximum height from one end of the tetramer to the other, as illustrated by the lower panels in Figure 4J. The full width of a tetrasome is about 11 nm, as 2nm-thick DNA makes three quarters of a turn around a protein core with a diameter of about 7 nm. The maximum height occurs between the entry and exit points of the tetrasome.

The structure (cf. Figure 4J) would suggest a ~5 nm distance between the points of maximum height in both flipping configurations, which is slightly larger than the observed 3.6 nm. This difference is expected since the position coordinate that we measure is the centroid of the tetrasome, not its highest point, and slight shifts of the tetrasome position may occur.

To estimate the change in linking number in our images, a feasible path of the DNA is drawn in Figure 4K-L. Since multiple geometries could be drawn that are compatible with the AFM images, the linking number change between these two states cannot be determined exactly, but all feasible configurations have a change in linking number between 1.5 and 2, which is in excellent agreement with the previously found value of 1.7. Flipping has only two stable states, as opposed to sliding, where one would expect a continuous distribution of positions. We therefore conclude that a flipping motion is the most likely explanation for the observed tetrasome dynamics.

2.3.3 Loop formation during tetrasome dissociation

Another interesting example of tetrasome dynamics can be seen in Figure 5. The tetrasome (assembled by NAP1) shown there initially has a usual appearance, but during the recording of the video, a loop develops around the site of the tetrasome, while the protrusion of the tetrasome itself laterally shrinks in size. The formation of this loop is accompanied by a shortening of the long arm of DNA by ~21 nm and an increase of total visible DNA length by ~24 nm, assuming the loop consists of DNA. During the loop formation there are large changes in position of the part of the DNA that is not covered by the tetrasome. This can be seen in Figure 5B, where the DNA molecule appears split, which is an imaging artefact caused by the scanning nature of AFM images. In fact, the DNA changed position during the time needed to acquire the image and therefore appeared in a different spot in the top half of the image. The loop subsequently remained around the tetrasome for several minutes, although it did change shape and size in this time. Then, after a few frames in which the top of the loop appeared instable (e.g. Figure 5E), the loop suddenly opened up and transformed into a sharp bend, with small proteins on the inside of the bend, presumably histones. In this process, the shorter arm of the DNA grew by ~25 nm, suggesting that the loop consisted of DNA and the histones stayed attached to the bases on the left-hand side of the DNA. This bend was very stable, remaining essentially unchanged upon several minutes of continuous imaging. Miyagi et al [21] also saw loops form on the unfolding of a nucleosome, but in that case, the loop formed in the first step of unfolding, with a loop of DNA unwrapping from the complete histone octamer.

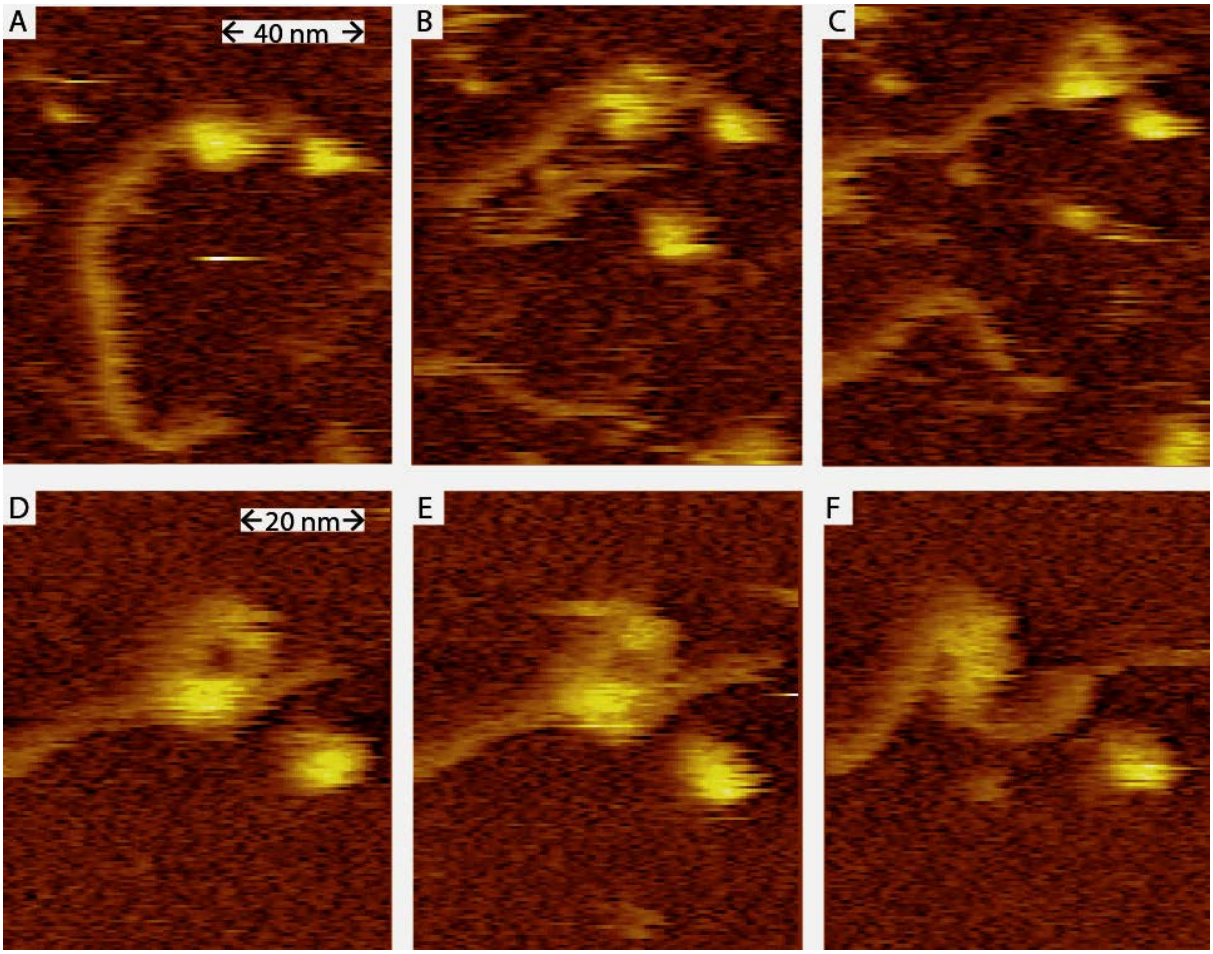

Figure 5: Loop formation upon tetrasome dissociation. A-C: Excerpts from a 246 frame AFM movie captured at 0.5 s per frame (Supplementary Movie 6). Non-consecutive frames showing respectively the tetrasome before, during and after formation of the loop. Time difference between A and B: 7.5 s, and between B and C: 3.5s. D-F Excerpts from a 973-frame AFM movie captured at 0.5 s per frame (Supplementary Movie 7). Non-consecutive frames respectively showing the loop before, during and after dissociation. Time between images is 2 s. The sharp bend seen in F essentially remains this way until the end of the movie.

The sharp bend with small features on the inside of the curve (see Figure 5F) is a motif that we often see in AFM images of NAP1-assembled tetrasomes or nucleosomes. The process observed in Figure 5 shows that these are remnants of dissociated tetrasomes. It should be noted that we see such sharp bends only in the presence of histone proteins, and not on samples prepared with only DNA, which indicates that these bends are protein-induced and not due to the increased bendability of DNA at short length scales [27]. The fact that histones can 'remember' the position of a previously formed tetrasome even though the tetrasome has fallen apart is remarkable, and whether this plays a role in nucleosome positioning *in vivo* is an interesting direction for future research.

3. Conclusion

In summary, we have observed the dynamics of nucleosomes and tetrasomes by high-speed Atomic Force Microscopy. We find that nucleosomes can spontaneously disassemble in a fast process (1 second timescale), that does not involve the formation of a DNA loop as an intermediate step. Tetrasomes disassemble spontaneously in this manner as well, but

for tetrasomes we also observed a process where a DNA loop approximately 25 nm in length is formed during the disassembly and remains stable for several minutes. On intact tetrasomes, we report sliding as well as reversible hopping between stable positions along the DNA. These results highlight the dynamic nature of (sub)nucleosomal structures that is important for a better understanding of the mechanisms by which nucleosomes are displaced and remodeled during transcription.

4. Experimental Section

AFM instrumentation: High-speed AFM measurements were performed with the RIBM HS-AFM 1.0 (RIBM co. ltd, Tsukuba, Japan). This instrument is very similar to that developed by Ando and co-workers [28, 29]. The measurements were performed either in the standard liquid cell with a volume of 120 µl, or in a home-built liquid cell with flow inlet and outlet, that has a volume of 12 µl. Both liquid cells are made of glass and the inert polymer PEEK. Quartz rods of 1.5 mm diameter and 2 mm height (Goodfellow, UK) were used as sample supports, and mica discs were attached to the supports with epoxy glue (Kombi Snel, Bison BV). The AFM cantilevers were NanoWorld USC-F1.2-k.015 or USC-F1.5-k0.6. These cantilevers have resonance frequencies in liquid between 350 and 650 kHz, and nominal spring constants of 0.15 and 0.6 N m-1 respectively. The tips of these cantilevers consist of High Density Carbon, made by Electron-Beam-Induced Deposition.

All AFM measurements were performed in the Amplitude Modulation mode of imaging (also known as 'tapping' mode). To minimize the influence of the AFM tip on the measurements, the oscillation amplitude was kept as close as possible to the unperturbed amplitude, which was in the range between 1 and 3 nm. To maintain a gentle setpoint despite variations in the drive efficiency and optical sensitivity, the second harmonic of the oscillation was monitored [30, 31]. Using either manual adjustment or automated electronic feedback, the drive amplitude was adjusted to keep amplitude of the second harmonic typically around 0.5%, and at least below 2% of the oscillation amplitude.

Surface preparation and buffer conditions: Mica is the preferred substrate for AFM imaging of DNA because of its extremely low surface roughness (<0.1 nm peak-to-valley) and the ease of preparing a clean surface. To achieve high-resolution imaging of DNA by AFM, DNA is typically attached to freshly cleaved mica via divalent ions in solution [32] or via chemical modification with amine-terminated silane groups [33]. The silane method is not suitable for observing dynamics of DNA-histone complexes, as this attaches the DNA rigidly to the substrate surface, reducing the accessibility and mobility of the DNA. Using divalent ions for the imaging of NAP1-assisted assembly of nucleosomes would imply an important deviation from protocols used in biochemical assays and magnetic tweezers experiments. Furthermore, the presence of Mg2+ ions in solution tends to accelerate aggregation of nucleosomes.

We found that, in contrast to widespread belief, DNA does adhere to mica in a buffer also without divalent ions, in a HEK buffer with 25 mM HEPES-KOH (pH 7.6), 50 mM KCl and 0.1 mM EDTA, see Figure 6(A-C). It has been noted before that HEPES can promote DNA surface adhesion in presence of Mg2+ [34]. Vanderlinden [35], recently reported that Potassium, but not Sodium, can mediate DNA adsorption to mica. However, without further surface preparation we found that DNA imaged in HEK buffer is only very loosely adhered and displays too much surface mobility to allow quantitative image analysis (Figure 6A-C). Therefore we use the long established, but less commonly used method of pre-incubating the mica with Mg2+ [36]. We found that the following protocol worked satisfactorily (a much simpler than the protocol used by Vesenka et al.): immediately after cleaving, a drop of 200 mM $MgCl_2$ is applied to the mica and incubated for 1 minute. The surface is then rinsed with pure water and dried in a

stream of nitrogen. Immediately after this, the sample of interest is deposited on the surface. Samples were incubated for 30-300 s depending on concentration, desired surface coverage and DNA length. After the incubation time, the surface is washed gently with imaging buffer, and transferred to the liquid cell. We find that DNA on mica treated in this way has a mobility that is slightly higher compared to DNA imaged on untreated mica in buffers containing 2 mM $MgCl_2$.

In early experiments, mica-supported lipid bilayers with a mixture of zwitterionic and positively charged lipids were investigated as an alternative to the bare surface of mica. Such bilayers have the advantage of a precisely tuneable charge density via variation of the mixing ratio, as well as low protein adsorption. These surfaces were prepared as follows: The zwitterionic lipid 1,2-dioleoyl-sn-glycero-3-phosphocholine (DOPC) and the positively charged lipid 1,2-dioleoyl-sn-glycero-3-ethylphosphocholine (18:1 EPC, chloride salt) were purchased from Avanti Polar Lipids as chloroform solutions and used as received. These lipids have a melting temperature of -20°C and thus are in the liquid-disordered phase at room temperature. The solutions were mixed in a glass vial in the desired ratio and the bulk of the solvent was evaporated by blowing dry nitrogen over the top of the vial, leaving a thin film of lipid at the bottom. The remaining solvent was evaporated by putting the vials in vacuum (10-3 mbar range) for 1 hour or longer. Lipids were then rehydrated in a buffer containing 100 mM KCl and 50 mM HEPES to a total lipid concentration of 1mM and vortexed. Liposome formation was achieved by bath

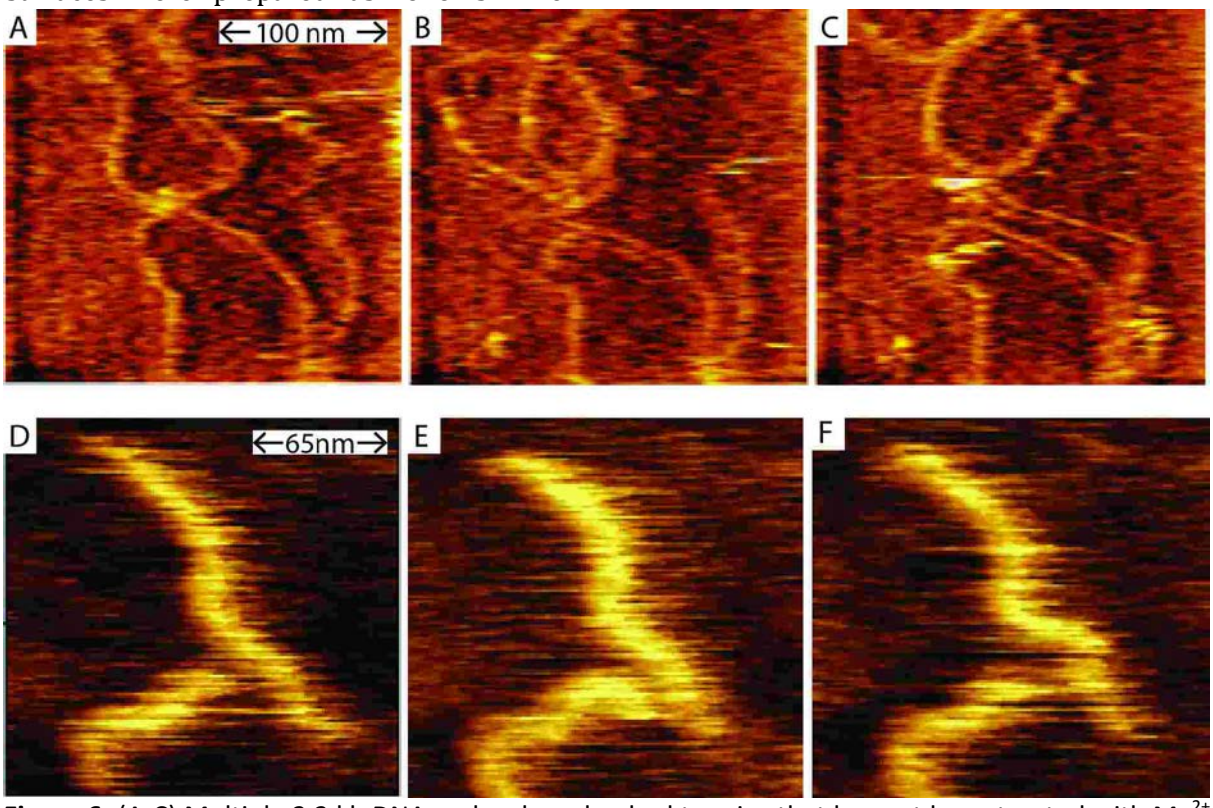

Figure 6: (A-C) Multiple 2.2 kb DNA molecules adsorbed to mica that has not been treated with Mg^{2+} ions, in HEK buffer. Three consecutive images are shown, taken at an acquisition speed of 0.4 s/frame. Without pre-treatment, the DNA is adsorbed to the surface, but extremely mobile. (D-F) Two 595 bp DNA molecules adsorbed to mica that was pre-treated with $MgCl_2$ as described in the main text. With pre-treatment, subtle movements of the DNA can be seen, but the overall position of the molecules is stable. Three consecutive images are shown, taken at an acquisition speed of 1 s/frame. To limit tip influence on DNA motion, the images were taken at very low applied force, which explains the relative lack of sharpness.

sonication for 30 mins, or as long as necessary to achieve a clear suspension. Liposome solution was applied to the mica surface, and incubated for 10 minutes to allow bilayer formation through spontaneous vesicle disruption onto the surface. Excess vesicles were then washed off the surface with imaging buffer.

Although some successful imaging was achieved for nucleosomes on these surfaces (see Figure 1), the preparation of the bilayers was not reliable enough for routine use. Specifically, it is difficult to tell from the AFM images whether a complete, defect-free bilayer has formed, or no bilayer has formed at all, since both situations lead to a surface with no discernable features. Only partially formed bilayers (or bilayers with small holes in them) can be positively identified in situ. When the bilayer is dried out after measurements, the lipid detaches from the surface in many places, migrates onto still attached parts of the bilayer and forms multilayer islands. If the surface is imaged in air immediately after drying, these lipid islands are the proof that a complete bilayer was present before the drying. Since we found that, firstly, the stability of nucleosomes on charged bilayers was not noticeably different from that on bare mica surfaces, and, secondly, the success of bilayer formation was both low and difficult to confirm before nucleosome deposition, this method was abandoned.

Due to the importance of macromolecular crowding for long-term stability of the nucleosomes, we investigated the feasibility of performing AFM measurements in the presence of crowding agents. BSA is a protein that is often used for crowding, but it is also well known as a surface passivation protein. It is therefore not surprising that in the presence of BSA, AFM imaging of DNA is nearly impossible. The BSA makes a dense layer on the mica surface, causing a high surface roughness and preventing DNA adsorption. Another agent used for crowding is the combination of Polyethylene Glycol (PEG) and Polyvinyl Alcohol (PVOH). We investigated HEK buffers with concentrations up to 2.3 % PEG, 2.3 % PVOH (w/v). We found that imaging of DNA by AFM is possible in all these concentrations. PEG/PVOH has low affinity for the mica surface, and does not prevent DNA adsorption. In the presence of PEG/PVOH, the images are noisier, however, presumably because macromolecules are caught between tip and surface for durations shorter than a scan line, leading to apparent height changes without spatial or temporal correlation.

Nucleosome and tetrasome assembly through salt dialysis: The assembly of nucleosomes and tetrasomes through salt dialysis is a well-established method [37, 38]. Histones and DNA are mixed together in a buffer containing a high concentration of salt. The high salt concentration screens the electric charges of the histones and the DNA backbone, preventing non-specific binding. By slowly reducing the salt concentration, first histones H3-H4 bind to the DNA. By even further reduction of the salt concentration, also histones H2A-H2B will bind to the tetrasomes. There are two critical points in the assembly process: One, a slow speed of the salt reduction: reducing the salt concentration too fast will lead to aggregation. Two, the ratio between DNA and histone concentrations needs to be set very precisely: too many histones will lead to non-specific binding and aggregation, while too few histones will result in inefficient assembly. In order to acquire regular nucleosome arrays, the total mass of DNA and histones should be nearly equal. To position nucleosomes at certain locations along the DNA, nucleosome positioning sequences such as the artificial 601-sequence (Widom sequence)[39] or the positioning sequence from the Xenopus borealis 5S rRNA gene [40] may be used. We assembled nucleosomes and tetrasomes both in the presence and absence of the 601-sequence during a 3-day salt dialysis at 4°C (see detailed description in Supplementary Information).

NAP1-assisted tetrasome and nucleosome assembly for AFM scanning: To optimize imaging conditions, we tried several assembly conditions. The conditions

used in other single-molecule experiments [11] contained BSA, which induces a large background noise. Leaving out all crowding agents (BSA, PEG, PVOH) resulted in only sparse histone binding to the DNA, and not in complete tetrasomes or nucleosomes. Optimal results were obtained when 0.37μM NAP1 was preincubated with 1.10μM histones for 24 hours at 4°C in a buffer containing 25mM Hepes-KOH (pH 7.6), 0.1mM Ethylenediaminetetraacetic acid (EDTA), 50mM KCl and 2.5%PEG and 2.5%PVOH (no BSA), followed by the addition of DNA without nucleosome positioning sequences (depending on the purpose of the measurement 1-5 tetrasomes/nucleosomes per DNA molecule). DNA was incubated for 8 hours. Right before the sample was placed on the mica, it was diluted 20 times to achieve the desired surface density.

Protein expression and purification was carried out as follows: Recombinant *Drosophila* core histones were expressed in *E. coli* Bl21(DE3) Rosetta (Novagen) and purified as described in Ref. [41]. The purification procedure for the H3/H4 dimers was identical to that of the H2A/H2B dimers. Expression plasmids were a kind gift of J. Kadonaga. Concentrations of core histones were determined by SDS PAGE and Coomassie staining. Recombinant *Drosophila* NAP1 was purified according to Ref. [42].

Data analysis methods: AFM images were analysed with custom written MatLab® (The Math Works, Inc.) scripts. In some cases, Gwyddion [43] was used for extracting feature sizes and heights in individual images. Because the high-speed AFM does not correct nonlinearity in the piezo elements during acquisition, AFM scanners were calibrated at several scan sizes using a 2D crystal of streptavidin molecules on a lipid bilayer [44]. A second-order polynomial was fitted to the scan size versus applied voltage curves, which was used to correct image sizes in post-processing. Standard plane and line-by-line background subtraction was used to obtain a flat background. For feature tracking, local maxima were identified and sub-pixel localization was achieved via a centre-of-mass algorithm. Full-image cross-correlation drift correction was used to minimize the effect of drift and shifts in the positioning of the imaging field. Where static objects could be identified, their positions were used to refine drift correction. Time traces of individual features were extracted from image series using elements of the UTrack MatLab package [45].

Supporting Information

The AFM movies of which single frames appear in Figures 1-6, and extended experimental protocols are available as Supplementary Information from the Wiley Online Library or from the author.

Acknowledgements

We are grateful to Susanne Hage, Bronwen Cross and Jaco de Groot for assistance in creating DNA constructs, and Jacob Kerssemakers for assistance with image processing. This work was supported by the ERC Advanced grant NanoforBio (no. 247072) and by the Netherlands Organisation for Scientific Research (NWO/OCW), as part of the Frontiers of Nanoscience program and by NanoNextNL, a micro and nanotechnology consortium of the Government of the Netherlands and 130 partners. A.L. acknowledges Austrian Science Fund (FWF) grant nr START Y275-B12.

References

1. Luger, K.; Mader, A. W.; Richmond, R. K.; Sargent, D. F.; Richmond, T. J., *Nature* **1997,** *389* (6648), 251-60. DOI 10.1038/38444.
2. Akey, C. W.; Luger, K., *Current opinion in structural biology* **2003,** *13* (1), 6-14. DOI http://dx.doi.org/10.1016/S0959-440X(03)00002-2.
3. Clapier, C. R.; Cairns, B. R., *Annual review of biochemistry* **2009,** *78*, 273-304. DOI 10.1146/annurev.biochem.77.062706.153223.
4. Li, G.; Levitus, M.; Bustamante, C.; Widom, J., *Nature structural & molecular biology* **2005,** *12* (1), 46-53. DOI 10.1038/nsmb869.
5. Jin, J.; Cai, Y.; Li, B.; Conaway, R. C.; Workman, J. L.; Conaway, J. W.; Kusch, T., *Trends in biochemical sciences* **2005,** *30* (12), 680-7. DOI 10.1016/j.tibs.2005.10.003.

6. Kimura, H., *DNA repair* **2005,** *4* (8), 939-50. DOI 10.1016/j.dnarep.2005.04.012.
7. Jackson, V., *Biochemistry* **1990,** *29* (3), 719-31.
8. van Holde, K. E.; Lohr, D. E.; Robert, C., *The Journal of biological chemistry* **1992,** *267* (5), 2837-40.
9. Mazurkiewicz, J.; Kepert, J. F.; Rippe, K., *The Journal of biological chemistry* **2006,** *281* (24), 16462-72. DOI 10.1074/jbc.M511619200.
10. Nakagawa, T.; Bulger, M.; Muramatsu, M.; Ito, T., *The Journal of biological chemistry* **2001,** *276* (29), 27384-91. DOI 10.1074/jbc.M101331200.
11. Vlijm, R.; Smitshuijzen, J. S.; Lusser, A.; Dekker, C., *PloS one* **2012,** *7* (9), e46306. DOI 10.1371/journal.pone.0046306.
12. Brower-Toland, B. D.; Smith, C. L.; Yeh, R. C.; Lis, J. T.; Peterson, C. L.; Wang, M. D., *Proceedings of the National Academy of Sciences of the United States of America* **2002,** *99* (4), 1960-5. DOI 10.1073/pnas.022638399.
13. Chien, F. T.; van Noort, J., *Current pharmaceutical biotechnology* **2009,** *10* (5), 474-85.
14. van Loenhout, M. T.; de Grunt, M. V.; Dekker, C., *Science* **2012,** *338* (6103), 94-7. DOI 10.1126/science.1225810.
15. Binnig, G.; Quate, C. F.; Gerber, C., *Physical review letters* **1986,** *56* (9), 930-933.
16. Hansma, P. K.; Cleveland, J.; Radmacher, M.; Walters, D.; Hillner, P.; Bezanilla, M.; Fritz, M.; Vie, D.; Hansma, H. G.; Prater, C.; others, *Applied Physics Letters* **1994,** *64*, 1738-1740.
17. Bucceri, A.; Kapitza, K.; Thoma, F., *The EMBO journal* **2006,** *25* (13), 3123-32. DOI 10.1038/sj.emboj.7601196.
18. Ando, T.; Uchihashi, T.; Kodera, N., *Annual review of biophysics* **2013,** *42*, 393-414. DOI 10.1146/annurev-biophys-083012-130324.
19. Katan, A. J.; Dekker, C., *Cell* **2011,** *147*, 979-82. DOI 10.1016/j.cell.2011.11.017.
20. Suzuki, Y.; Higuchi, Y.; Hizume, K.; Yokokawa, M.; Yoshimura, S. H.; Yoshikawa, K.; Takeyasu, K., *Ultramicroscopy* **2010,** *110* (6), 682-8. DOI 10.1016/j.ultramic.2010.02.032.
21. Miyagi, A.; Ando, T.; Lyubchenko, Y. L., *Biochemistry* **2011,** *50*, 7901-8. DOI 10.1021/bi200946z.
22. Davey, C. A.; Sargent, D. F.; Luger, K.; Maeder, A. W.; Richmond, T. J., *Journal of molecular biology* **2002,** *319* (5), 1097-113. DOI 10.1016/S0022-2836(02)00386-8.
23. Hamiche, A.; Carot, V.; Alilat, M.; De Lucia, F.; O'Donohue, M. F.; Revet, B.; Prunell, A., *Proceedings of the National Academy of Sciences of the United States of America* **1996,** *93* (15), 7588-93.
24. Levchenko, V.; Jackson, B.; Jackson, V., *Biochemistry* **2005,** *44* (14), 5357-72. DOI 10.1021/bi047786o.
25. Liu, L. F.; Wang, J. C., Proceedings of the National Academy of Sciences of the United States of America **1987,** 84 (20), 7024-7.
26. Vlijm, R., Lee, M., Lipfert, J., Lusser, A., Dekker, C. and Dekker, N.H., **Submitted**.
27. Wiggins, P. A.; van der Heijden, T.; Moreno-Herrero, F.; Spakowitz, A.; Phillips, R.; Widom, J.; Dekker, C.; Nelson, P. C., *Nature nanotechnology* **2006,** *1* (2), 137-41. DOI 10.1038/nnano.2006.63.
28. Ando, T.; Uchihashi, T.; Fukuma, T., *Progress in Surface Science* **2008,** *83*, 337-437. DOI 10.1016/j.progsurf.2008.09.001.
29. Uchihashi, T.; Kodera, N.; Ando, T., *Nature protocols* **2012,** *7*, 1193-206. DOI 10.1038/nprot.2012.047.
30. Kodera, N.; Sakashita, M.; Ando, T., *Review of Scientific Instruments* **2006,** *77*, 083704. DOI 10.1063/1.2336113.
31. Schiener, J.; Witt, S.; Stark, M.; Guckenberger, R., *Review of Scientific Instruments* **2004,** *75*, 2564. DOI 10.1063/1.1777405.
32. Hansma, H. G.; Laney, D. E., *Biophysical journal* **1996,** *70*, 1933-9. DOI 10.1016/S0006-3495(96)79757-6.
33. Lyubchenko, Y. L., *Micron (Oxford, England : 1993)* **2010,** *42*, 196-206. DOI 10.1016/j.micron.2010.08.011.
34. Bezanilla, M.; Manne, S.; Laney, D. E.; Lyubchenko, Y. L.; Hansma, H. G., *Langmuir : the ACS journal of surfaces and colloids* **1995,** *11*, 655-659. DOI 10.1021/la00002a050.
35. Vanderlinden, W., Quantitative Scanning Force Microscopy of the loops and curls in DNA., Ph.D. Thesis, KU Leuven, **2012**.
36. Vesenka, J.; Guthold, M.; Tang, C. L.; Keller, D.; Delaine, E.; Bustamante, C., *Ultramicroscopy* **1992,** *42-44*, 1243-1249. DOI 10.1016/0304-3991(92)90430-R.
37. Luger, K.; Rechsteiner, T. J.; Richmond, T. J., *Methods in enzymology* **1999,** *304*, 3-19.
38. Lee, K.-M.; Narlikar, G., Assembly of Nucleosomal Templates by Salt Dialysis. In *Current Protocols in Molecular Biology*, John Wiley & Sons, Inc.: 2001.
39. Lowary, P. T.; Widom, J., *Journal of molecular biology* **1998,** *276* (1), 19-42. DOI 10.1006/jmbi.1997.1494.
40. Hayes, J. J.; Tullius, T. D.; Wolffe, A. P., Proceedings of the National Academy of Sciences of the United States of America **1990,** 87 (19), 7405-9.
41. Levenstein, M. E.; Kadonaga, J. T., *The Journal of biological chemistry* **2002,** *277* (10), 8749-54. DOI 10.1074/jbc.M111212200.
42. Lusser, A.; Urwin, D. L.; Kadonaga, J. T., *Nature structural & molecular biology* **2005,** *12* (2), 160-6. DOI 10.1038/nsmb884.
43. Nečas, D.; Klapetek, P., *Central European Journal of Physics* **2012,** *10*, 181-188. DOI 10.2478/s11534-011-0096-2.
44. Yamamoto, D.; Nagura, N.; Omote, S.; Taniguchi, M.; Ando, T., *Biophysical journal* **2009,** *97*, 2358-67. DOI 10.1016/j.bpj.2009.07.046.
45. Jaqaman, K.; Loerke, D.; Mettlen, M.; Kuwata, H.; Grinstein, S.; Schmid, S. L.; Danuser, G., *Nat Methods* **2008,** *5*, 695-702. DOI 10.1038/nmeth.1237.

Supporting Information

Dynamics of nucleosomal structures measured by high-speed Atomic Force Microscopy

*Allard J. Katan, Rifka Vlijm, Alexandra Lusser and Cees Dekker**

Description of supplementary movies

Supplementary movie 1: Full AFM movie from which the images in Figure 1 in the main text are taken. Acquisition speed 1 s/frame, resolution 250x250 pixels, frame size 190 nm wide, 218 nm high.

Supplementary movie 2: Full AFM movie from which the images in Figure 2 in the main text are taken. Acquisition speed 1 s/frame, resolution 300x200 pixels, frame size 233 nm wide, 263 nm high.

Supplementary movie 3: Full AFM movie from which the images in Figure 3 are taken. Acquisition speed 1 s/frame, resolution 180x180 pixels, frame size 139 nm wide, 129 nm high.

Supplementary movie 4: Full AFM movie from which the images in Figure 4A-D in the main text are taken. Acquisition speed 1 s/frame, resolution 150x150 pixels, frame size 116 nm wide, 137 nm high.

Supplementary movie 5: Full AFM movie from which the images in Figure 4G-I in the main text are taken. Acquisition speed 0.3 s/frame, resolution 150x150 pixels, frame size 55 nm wide, 66 nm high.

Supplementary movie 6: Full AFM movie from which the images in Figure 5A-C in the main text are taken. Acquisition speed 0.5 s/frame, resolution 150x150 pixels, frame size 109 nm wide, 128 nm high.

Supplementary movie 7: Full AFM movie from which the images in Figure 5D-F in the main text are taken. Acquisition speed 0.5 s/frame, resolution 150x150 pixels, frame size 63 nm wide, 76 nm high.

Salt dialysis of nucleosomes

As described in the main text, the assembly of nucleosomes and tetrasomes through salt dialysis is a well-established method [37, 38]. First, the histones and DNA are mixed in a high salt buffer. Next, the salt concentration was slowly reduced, in our case over a time period of three days at 4°C. Finally the samples were stored until use in a low salt buffer at 4°C.

DNA constructs for salt dialysis of nucleosomes and tetrasomes

Mainly two constructs were used, with one or two copies of the nucleosome positioning sequence '601'[39]:

- 1027bp DNA, containing one 601-sequence (193bp linker, 553bp linker)
- 2284bp DNA, containing two 601 sequences, (20bp linker, 467 bp linker).

Histone octamers

Chicken-erythrocyte histone octamers were obtained from Abcam (#ab45275).

Buffers

It is important to make all the buffers fresh, since DTT and benzamidine become less active over time.

High salt buffer (250 ml)	20mM Tris-HCl (pH 7.5)	5ml of 1M stock
	1mM EDTA	0.5ml of 0.5M stock
	2M KCl	166.7ml of 3M stock
	1mM DTT	250 µl of 1M stock
	0.5mM Benzamidine	125 µl of 1M stock
	mQ	77.425ml
Low salt buffer (1L)	20mM Tris-HCl (pH 7.5)	20ml of 1M stock
	1mM EDTA	2 ml of 0.5M stock
	10mM KCl	3.33 ml of 3M stock
	1mM DTT	1 ml of 1M stock
	0.5mM benzamidine	0.5 ml 1M stock
	mQ	973.17 ml
Assembly buffer (1ml)	20mM Tris-HCl (pH 7.5)	20µl of 1M stock
	1mM EDTA	2 µl of 0.5M stock
	2M KCl	666.67µl of 3M stock
	10mM DTT	10µl of 1M stock
	0.5mM benzamidine	0.5µl of 1M Stock
	mQ	300.83µl

Protocol

Step 1: Place the buffers without DTT and benzamidine at 4°C. When the temperature of 4°C is reached, finish the buffers by adding DTT and benzamidine.

Step 2: Rinse the dialysis cups (Thermo Scientific, #69550; 3.5K-MWCO) in 50°C warm mQ water for 10 minutes and remove leaking cups. Cool down in cold mQ.

Step 3: Dilute abcam octamers 10 times to 0.175 mg/ml with assembly buffer, for higher pipetting precission. Use LoBind Eppendorf tubes to prevent protein loss due to sticking to the tubes.

Step 4: Prepare the histone-DNA mix. In our experiments, we do not aim for maximum number of nucleosomes, but instead only want one or two nucleosomes. For this purpose we prepared three different weight ratios of DNA:octamer of 1:0.3, 1:0.2 and 1:0.15. A total of 5µg of DNA, and 1.5/1.0 or 0.75µg of histone octamers was mixed in the assembly buffer to add up to a total volume of 40µl and each of the mixes was placed in a separate dialysis cup.

Step 5: Prepare the dialysis setup as shown in FigureS1. A 250ml beaker with stir bar should be filled with high salt buffer and placed on a stirrer in a cold room with a temperature of 4°C. Two clean tubes should be attached to the inner wall of this beaker such that the ends nearly touch the bottom of the beaker. One of these tubes should go to a beaker containing the low-salt buffer and the other should go to a waste container, with a minimum volume of a litre. A peristaltic pump (Ismatec) is set to pump low salt buffer into the dialysis beaker and, at the same rate, remove buffer from the dialysis beaker to the waste container.

Step 6: Place the dialysis cups in a floating device, and place this floating device into the beaker containing the high salt buffer. Start the stirring device and make sure the floater is free to rotate.

Step 7: Set the pump such that one litre is pumped over a time of 60 hours.

Step 8: When the dialysis is finished, write down the final volume in the individual dialysis cups and store the samples in a LoBind Eppendorf tube until use at 4°C.

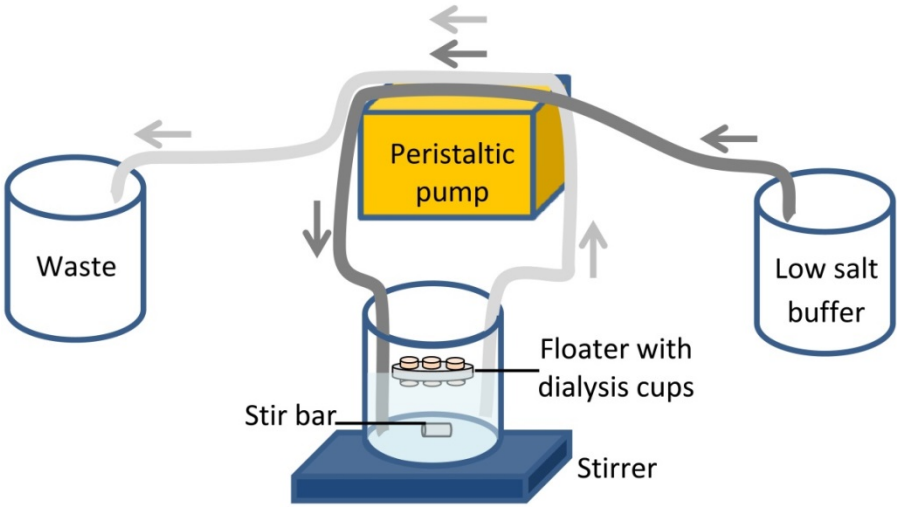

Figure S1: Schematic representation of the salt-dialysis setup. During a 60-hour dialysis at 4°C, the salt concentration is reduced from 2M to 10mM KCl.

Verification of assembly conditions in the absence of bovine serum albumin (BSA).

The presence of bovine serum albumin (BSA) in solution creates large problems for AFM experiments since a lot of BSA proteins appear on the surface upon AFM imaging. The buffer components BSA, Polyethylene Glycol (PEG) and Polyvinyl Alcohol (PVOH) support NAP1-mediated nucleosome and tetrasome assembly, as well as stabilize the formed (sub)nucleosomal structures. We verified several assembly conditions with and without BSA by use of bulk gel experiments. We found that NAP1-mediated assembly of tetrasomes is possible in the absence of BSA, provided that PEG and PVOH are present in the (pre)assembly buffer. An example of NAP1-assembled $(H3\text{-}H4)_2$ tetrasomes in the absence of BSA is shown in Figure S2. A detailed description of the NAP1-mediated assembly as well as the preparation of the gel is described below.

Protein buffer condition

- 25mM Hepes-KoH (pH 7.6)
- 0.1mM EDTA
- 50mM KCl_2
- 0.2% Polyethylene Glycol (PEG) (w/v)
- 0.2% Polyvinyl Alcohol (PVOH) (w/v)

DNA and proteins

- 250bp DNA (no nucleosome positioning sequence), stock concentration of 138 µg/ml (mW = 165kD).
- NAP1: stock concentration of 160µg/ml (mW = 43kD).
- Histones H3-H4 in equimolar mix, stock concentration of 9mg/ml (mW = 28kD).

Tetrasome assembly and gel imaging protocol

Step 1: Take the proteins and DNA and place them on ice.

Step 2: Make dilutions with the protein buffer. Dilute DNA 5 times and H3-H4 250 times, both in siliconised low-protein-binding tubes.

Step 3: Preincubate the proteins 30 minutes on ice:

	buffer	NAP1	Dil. H3-H4	Volume
Tube 1:	4.18 µl	0 µl	0 µl	4.18 µl
Tube 2:	2.58 µl	0.3 µl	1.3 µl	4.18 µl
Tube 3:	2.58 µl	0.3 µl	1.3 µl	4.18 µl

Step 4: During preincubation of the proteins, prerun a 6% Page gel (Novex® TBE precasted gel, #EC6265BOX) at 180V

Step 5: Add 1.087 µl of 5 times diluted 250bp DNA and incubate for 15 minutes on ice.

Step 6: Add 1.2µl 6X loading dye (Thermo Scientific, #R0611)

Step 7: Load tube 2 is loaded into lane 4, 5 minutes before tube 3 is loaded into lane 5 to verify that dilution does not significantly affect the stability of the tetrasomes on a short time scale.

Step 8: Load the other lanes: Lane 1 = 0.8µl bench top marker (Promega BenchTop 1kb DNA Ladder, #G7541), Lane 2 left empty, Lane 3: Tube 1 (bare 250bP DNA), Lane 5: Tube 3 (H3-H4 tetrasome).

Step 9: Run the gel for 1 hr and 10 minutes at 180V. (In Figure S2, due to an accidentally not completely closed lid, the gel only started to run 20 minutes after loading)

Step 10: Stain the gel with 1X Cybr Gold (Life Technologies, #S-11494) for half an hour, then wash the gel in 1X TBE for 10 minutes to reduce stains

Step 11: Image the gel using GE Healthcare Typhoon™.

Conclusion

Since a band around 1kbp was formed in all the lanes with 250bp DNA and NAP1 with tetramers (lanes 4 and 5), indeed NAP1-mediated tetrasome assembly is possible in the absence of BSA. Since the bare DNA band was clearly visible in lanes 4 and 5, a higher concentration of NAP1 and histones probably could increase the number of assembled tetrasomes. However, in this experiment we chose not to add an excess amount of proteins in order to reduce the protein background in the AFM imaging.

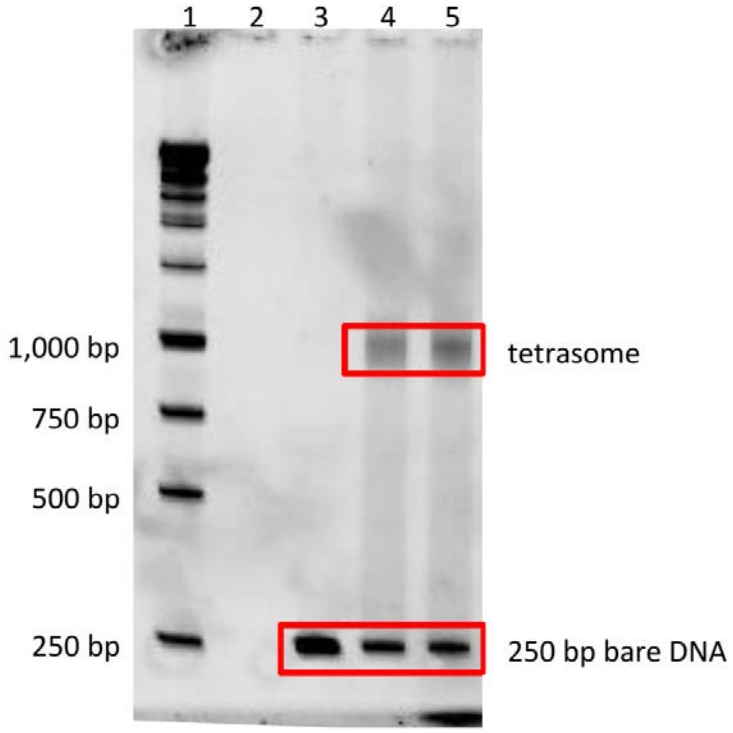

Figure S2: 6% Page TBE gel. Lane 1: bench top marker, Lane 3: bare 250 bp DNA, Lane 4 and 5: DNA with $(H3\text{-}H4)_2$ tetrasomes.